

29 Glitches Detected at Urumqi Observatory

J. P. Yuan,^{1,2} N. Wang,^{1*} R. N. Manchester³, Z. Y. Liu,¹

¹*Urumqi Observatory, NAOC, 40-5 South Beijing Road, Urumqi, Xinjiang, China, 830011*

²*Graduate University of the Chinese Academy of Sciences, 19A Yuquan road, Beijing, China, 100049*

³*Australia Telescope National Facility, CSIRO, PO Box 76, Epping, NSW 1710, Australia*

8 September 2018

ABSTRACT

Glitches detected in pulsar timing observations at the Nanshan radio telescope of Urumqi Observatory between 2002 July and 2008 December are presented. In total, 29 glitches were detected in 19 young pulsars, with this being the first detection of a glitch in 12 of these pulsars. Fractional glitch amplitudes range from a few parts in 10^{-11} to 3.9×10^{-6} . Three “slow” glitches are identified in PSRs J0631+1036, B1822–09 and B1907+10. Post-glitch recoveries differ greatly from pulsar to pulsar and for different glitches in the same pulsar. Three small glitches in PSRs B0402+61, B0525+21 and J1853+0545 show evidence for normal post-glitch recovery, but for PSRs B0144+59 and B2224+65 the spin frequency ν continually increases relative to the pre-glitch solution for hundreds of days after their small glitches. Most large glitches show some evidence for exponential post-glitch recovery on timescales of 100 – 1000 days, but in some cases, e.g., PSR B1758–23, there is little or no recovery, that is, no detectable increase in $|\dot{\nu}|$ at the time of the glitch. Beside exponential recoveries, permanent increases in slowdown rate are seen for the two large glitches in PSRs B1800–21 and B1823–13. These and several other pulsars also show a linear increase in $\dot{\nu}$ following the partial exponential recovery, which is similar to the Vela pulsar post-glitch behaviour. However, the rate of increase, $\ddot{\nu}$, is an order of magnitude less than for the Vela pulsar. We present improved positions for 14 of the glitching pulsars. Analysis of the whole sample of known glitches show that fractional glitch amplitudes are correlated with characteristic age with a peak at about 10^5 years, but there is a spread of two or three orders of magnitude at all ages. Glitch activity is positively correlated with spin-down rate, again with a wide spread of values. For some (but not all) pulsars there is a correlation between glitch amplitude and the duration of the following inter-glitch interval. In no case is there a correlation of glitch amplitude with the duration of the preceding inter-glitch interval.

Key words: methods: data analysis – stars: neutron – pulsar: general

1 INTRODUCTION

After allowing for the accurate determination of the pulsar spin-down, pulse arrival-time measurements display two types of irregularities in the pulsar rotation rate: timing noise and glitches. Timing noise is a continuous wandering of the pulsar rotation rate, on time-scales of days, months and years. In most young pulsars, timing noise is generally very “red”, i.e., stronger at lower frequencies (Cordes & Downs 1985), and the second time-derivative of the pulse frequency is commonly used as an indicator of the level of noise.

Glitches are characterized by a sudden increase in the pulsar rotation rate, often followed by a (partial) recovery toward the pre-glitch status. Glitches were first ob-

served in the Vela pulsar (Radhakrishnan & Manchester 1969; Reichley & Downs 1969) and it was soon realized that they could be an important diagnostic for studying neutron-star interiors (Ruderman 1969; Baym et al. 1969). It is widely believed that these events are caused by either sudden and irregular transfer of angular momentum from a faster rotating interior super-fluid to the solid crust of the neutron star, or quakes in a solid component of the star, or even both. The result is a sudden increase in the rotational frequency ν of the pulsar with a relative magnitude normally in the range $10^{-10} < \Delta\nu_g/\nu < 5 \times 10^{-6}$. Large glitches ($\Delta\nu_g/\nu > 10^{-7}$) are usually accompanied by jumps in the spin-down rate ($\Delta\dot{\nu}_g/\dot{\nu} \sim 10^{-4}$ to 10^{-2}). A characteristic feature of many glitches is a relaxation after the frequency jump, which may occur over periods of minutes to years. In some cases, this relaxation is approximately expo-

* E-mail: na.wang@uao.ac.cn

nential toward the extrapolated pre-glitch state, but many different forms of relaxation are observed, some with multiple timescales. Lyne et al. (2000) presented evidence that the degree of relaxation in different pulsars is related to their spin-down rate $|\dot{\nu}|$.

Although glitches are a rather rare phenomena, an increasing number of these events have been reported (Wang et al. 2000; Krawczyk et al. 2003; Janssen & Stappers 2006), permitting more comprehensive statistical studies (e.g., Lyne et al. 2000). To date about 170 glitches have been observed, in 51 of the over 1800 known pulsars¹. The most frequent glitches have been detected in PSRs B0531+21 (Crab), J0537–6910, B0833–45 (Vela), J1341–6220 and B1737–30, which have characteristic ages in the range $\sim 10^3$ to 10^5 yr. PSR J0537–6910 has glitched 23 times in seven years, with most of the glitches being relatively small in $\Delta\nu_g/\nu$ terms (typically a few parts in 10^{-7}). Their amplitude shows a strong correlation with the interval to the following glitch (Middlethick et al. 2006). Glitches in the Crab pulsar are even smaller, with $\Delta\nu_g/\nu$ typically $\sim 10^{-9}$ (Lyne et al. 1993). There is normally a rapid exponential decay over several days and a persistent increase in slow-down rate (Lyne et al. 1993). The Vela pulsar is the prototypical pulsar showing large glitches, with $\Delta\nu_g/\nu$ generally $> 10^{-6}$ although some small and intermediate-sized glitches have been observed. The post-glitch decay is initially exponential, with evidence for several timescales ranging from 1 minute to several hundred days, but subsequently linear till the next glitch (Dodson et al. 2007; Lyne et al. 1996). PSR B1737–30 is a frequently glitching pulsar which shows a large range of glitch sizes and a high value of the glitch activity parameter

$$A_g = \frac{1}{T} \sum \frac{\Delta\nu_g}{\nu}, \quad (1)$$

where T is the total data span (McKenna & Lyne 1990; Shemar & Lyne 1996; Zou et al. 2008). Significant post-glitch decays are observed for the larger glitches.

Clearly, the glitch phenomenon in pulsars is complex. Further observations of a larger sample of pulsars will help to quantify and understand processes responsible for the very different glitch and post-glitch behaviours observed both between different pulsars and in different glitches in the same pulsar.

Nearly 280 pulsars are being monitored regularly at Urumqi Observatory in a timing program which commenced in 2000. The aims of the project are to make precise measurements of the position and timing behaviour of pulsars, to provide ephemeris for observations at radio and other wavelengths (e.g., Smith et al. 2008) and to investigate the interiors of neutron stars by monitoring irregularities in their rotation behaviour. In this paper we describe the glitches detected in our observations, together with updated descriptions of the relaxations for some previously reported glitches.

2 OBSERVATIONS AND ANALYSIS

Timing observations of pulsars using the Urumqi Observatory 25-m radio telescope at Nanshan started in 2000 January with a dual-channel room-temperature receiver. A dual-channel cryogenic receiver system has been used at the central observing frequency of 1540 MHz since 2002 July. Approximately 280 pulsars are observed regularly three times each month and results to 2008 December are reported here. The two polarizations, each of bandwidth 320 MHz, are sent to a filter-bank consisting of 2×128 channels of width 2.5 MHz. The data are digitized to one-bit precision, and the integration time is typically 4 to 16 min (Wang et al. 2001).

Off-line data reduction was performed in the following steps. The data for each pulsar were dedispersed and summed to produce a total intensity profile centered at 1540 MHz. Local arrival times were determined by correlating the data with standard pulse profiles; the pulse times of arrival (TOAs) normally correspond to the peak of the main pulse. TOAs at the Solar-system barycenter were obtained using the standard timing program TEMPO² with the Jet Propulsion Laboratories DE405 ephemeris (Standish 1998). A model for the pulsar timing was fitted to these barycentric TOAs, weighted by the inverse square of their uncertainty. Errors in the fitted parameters are taken to be twice the standard errors obtained from TEMPO. The basic timing model for the barycentric pulse phase, ϕ , as a function of time t , is

$$\phi(t) = \phi_0 + \nu(t - t_0) + \frac{1}{2}\dot{\nu}(t - t_0)^2 + \frac{1}{6}\ddot{\nu}(t - t_0)^3, \quad (2)$$

where ϕ_0 is the phase at time t_0 and ν , $\dot{\nu}$, $\ddot{\nu}$ represent the pulse frequency, frequency derivative and frequency second derivative respectively. Pulsar positions were derived from long inter-glitch intervals with the residuals being “whitened” by fitting of higher-order frequency derivatives if necessary.

Glitches can be described as combinations of steps in ν and $\dot{\nu}$, of which parts may decay exponentially on various timescales. We assume a glitch model for the observed phenomenon as below:

$$\nu(t) = \nu_0(t) + \Delta\nu_p + \Delta\dot{\nu}_p t + \Delta\nu_d e^{-t/\tau_d} \quad (3)$$

$$\dot{\nu}(t) = \dot{\nu}_0(t) + \Delta\dot{\nu}_p + \Delta\dot{\nu}_d e^{-t/\tau_d} \quad (4)$$

where $\Delta\nu_p$ and $\Delta\dot{\nu}_p$ are, respectively, the permanent changes in frequency and frequency derivative relative to the pre-glitch values and $\Delta\nu_d$ is the amplitude of the exponential recovery with a decay time constant of τ_d . We note that for glitches the jump in frequency ν is positive and the jump in frequency derivative $\dot{\nu}$ is usually negative. Since $\dot{\nu}$ is negative, a negative jump corresponds to an increase in magnitude of the spin-down rate. The total frequency change at the glitch is

$$\Delta\nu_g = \Delta\nu_p + \Delta\nu_d. \quad (5)$$

The degree of recovery is often described by the parameter Q :

$$Q = \Delta\nu_d/\Delta\nu_g. \quad (6)$$

¹ See the ATNF Pulsar Catalogue (Manchester et al. 2005) Glitch table at www.atnf.csiro.au/research/pulsar/psrscat

² See <http://www.atnf.csiro.au/research/pulsar/tempo>

Table 1. Parameters for the pulsars with observed glitches

Pulsar Name		RA (h m s)	Dec (d m s)	Epoch MJD	P (s)	\dot{P} (10^{-15})	Age (kyr)	B_s (10^{12} G)	References for position
J0147+5922	B0144+59	01:47:44.6457(17)	+59:22:03.293(15)	53160	0.1963	0.256	12100.0	0.23	this work
J0406+6138	B0402+61	04:06:30.082(3)	+61:38:41.04(3)	53784	0.5945	5.576	1690.0	1.84	this work
J0528+2200	B0525+21	05:28:52.264(9)	+22:00:04(2)	53100	3.7455	40.036	1480.0	12.40	this work
J0631+1036		06:31:27.524(4)	+10:37:02.5(3)	53850	0.2877	104.683	43.6	5.55	this work
J1705-3423		17:05:42.363(3)	-34:23:45.17(12)	53830	0.2554	1.075	3760.0	0.53	this work
J1740-3015	B1737-30	17:40:33.82(1)	-30:15:43.5(2)	52200	0.6068	466.358	20.6	17.00	1
J1751-3323		17:51:32.725(11)	-33:23:39.6(9)	53750	0.5482	8.897	976.0	2.23	this work
J1801-2304	B1758-23	18:01:19.829(3)	-23:04:44.2(2)	50809	0.4158	112.880	58.4	6.93	2
J1803-2137	B1800-21	18:03:51.411(1)	-21:37:07.35(1)	51544	0.1336	134.100	15.8	4.28	3
J1812-1718	B1809-173	18:12:07.208(8)	-17:18:29.5(11)	49612	1.2053	19.770	1000.0	4.85	4
J1818-1422	B1815-14	18:18:23.7660(17)	-14:22:36.71(16)	54000	0.2914	2.038	2270.0	0.78	this work
J1825-0935	B1822-09	18:25:30.629(6)	-09:35:22.3(3)	53300	0.7689	52.285	233.0	6.42	this work
J1826-1334	B1823-13	18:26:13.175(3)	-13:34:46.8(1)	52400	0.1015	75.061	21.4	2.79	this work
J1841-0425	B1838-04	18:41:05.663(1)	-04:25:19.50(7)	53900	0.1861	6.391	461.0	1.10	this work
J1853+0545		18:53:58.411(1)	+05:45:55.26(3)	53882	0.1264	0.611	3280.0	0.28	this work
J1902+0615	B1900+06	19:02:50.277(2)	+06:16:33.41(6)	53390	0.6735	7.706	1380.0	2.31	this work
J1909+1102	B1907+10	19:09:48.694(2)	+11:02:03.35(3)	49912	0.2836	2.639	1700.0	0.88	4
J1915+1009	B1913+10	19:15:29.984(2)	+10:09:43.67(4)	53300	0.4045	15.251	420.0	2.51	this work
J2225+6535	B2224+65	22:25:52.721(7)	+65:35:35.58(4)	53880	0.6825	9.659	1130.0	2.58	this work

1 Fomalont et al. (1997); 2. Frail et al. (1993); 3. Brisken et al. (2006); 4. Hobbs et al. (2004).

Because of the decaying component, the instantaneous change in $\dot{\nu}$ at the glitch differs from $\Delta\dot{\nu}_p$

$$\Delta\dot{\nu}_g = \Delta\dot{\nu}_p + \Delta\dot{\nu}_d = \Delta\dot{\nu}_p - Q\Delta\nu_g/\tau_d \quad (7)$$

Solutions before and after the glitch are used to estimate the steps in frequency and its derivative. If the gap between observations around the glitch is not too large, the glitch epoch can be estimated more accurately by requiring a phase-connected solution over the gap in the TEMPO fit. However if the gap is too large, rotations can be missed and the glitch epoch is estimated as the mid-point of the gap between observations around the glitch.

3 RESULTS

We present the results of glitch analysis using Nanshan timing data from July 2002 to Dec 2008. Table 1 lists the parameters for the 19 pulsars for which glitches were observed. The first two columns give the pulsar names based on J2000 and B1950 coordinates and the third and fourth columns are their J2000 positions. The next four columns give the pulsar period and period derivative, characteristic age $\tau_c = P/(2\dot{P})$ and surface dipole magnetic field $B_s = 3.2 \times 10^{19} \sqrt{P\dot{P}}$ G. Most of the positions quoted in Table 1 result from our work except for five pulsars where the referenced positions are more accurate. Estimated uncertainties in the last quoted digit, given in brackets, are 2σ from the TEMPO fit in this and following tables. References for the position are given in the final column. The data spans used to determine the positions are the largest available which are not too strongly affected by post-glitch recovery. Typical spans are 3 – 5 yr, with a minimum of 2.3 yr and a maximum of 7.5 yr.

As mentioned in Section 2 the data sets used for position fitting are whitened by fitting for higher order derivatives of frequency. In most cases, five or less derivatives are sufficient to whiten the data, giving rms residuals of 100 – 700 μ s. For PSR J1751-3323, nine derivatives were required and for PSR B1815-14, seven derivatives. Zou et al. (2005) investigated the effect of timing noise on the determination of pulsar positions, showing that an uncertainty of twice the formal TEMPO error is generally realistic for data spans of the order of 5 yr.

In total, 29 glitches were detected in these pulsars. The rotational parameters from independent fits to the pre-glitch and post-glitch data are given in Table 2. Except for short sections of data, the fits include a $\ddot{\nu}$ term, which is generally dominated by timing noise or recovery from a previous glitch.

Glitch parameters are given in Table 3, in which the second column gives the glitch epoch, and the next two columns give the fractional changes in ν and $\dot{\nu}$ at the glitch determined by extrapolating the pre- and post-glitch solutions to the glitch epoch. Quoted uncertainties include a contribution from the uncertainty in glitch epoch. Results of directly fitting for the glitch parameters in TEMPO are given in the remaining columns. Decay terms were only fitted when significant decay was observed.

The rotational behaviour of these pulsars are shown in Fig. 1 to 21. Values of ν and $\dot{\nu}$ were obtained from independent fits of Equation 2 (omitting the $\ddot{\nu}$ term) to data spans ranging from 50 d to 200 d. The residual frequencies have been obtained at the various epochs by the subtraction of the pre-glitch models. We discuss the results for each pulsar in the following Sections.

Table 2. Pre- and post-glitch timing solutions

Pulsar Name	ν (s^{-1})	$\dot{\nu}$ (10^{-12} s^{-2})	$\ddot{\nu}$ (10^{-24} s^{-3})	Epoch (MJD)	MJD Range	No. of TOAs	RMS (μs)
B0144+59	5.093689334287(4)	-0.0066633(2)	—	53160.0	52486–53662	90	101
	5.093688844679(4)	-0.0066619(2)	—	54011.0	53686–54831	107	145
B0402+61	1.68187172559(1)	-0.015757(2)	—	52745.0	52469–53022	57	395
	1.681870311647(2)	-0.01576474(8)	—	53784.0	53050–54830	189	541
B0525+21	0.266984828978(2)	-0.0028537(3)	—	51864.0	51546–52271	85	575
	0.266984598507(1)	-0.00285481(3)	—	52800.0	52287–53975	249	834
	0.266984253314(2)	-0.0028550(1)	—	54200.0	53982–54831	182	817
J0631+1036	3.47486317481(6)	-1.263638(6)	30(2)	52657.0	52473–52842	40	274
	3.47482575938(6)	-1.265058(9)	106(1)	53000.0	52853–53219	37	685
	3.474732970746(8)	-1.263032(1)	5.47(8)	53850.0	53238–54100	175	1454
	3.47467842199(3)	-1.263630(2)	15.7(6)	54350.0	54129–54630	106	5003
	3.4746348982(1)	-1.26374(2)	166(12)	54750.0	54634–54831	57	315
J1705–3423	3.915021810541(8)	-0.0164948(2)	—	53800.0	52486–54384	222	670
	3.9150208150(1)	-0.016495(9)	—	54500.0	54394–54832	44	590
B1737–30	1.647839443329(3)	-1.2659499(3)	13.16(9)	54000.0	53101–54394	115	1962
	1.64778155382(3)	-1.26561(1)	59(3)	54530.0	54463–54685	19	314
	1.6477542263(1)	-1.26557(3)	—	54780.0	54695–54808	7	338
J1751–3323	1.82406604540(3)	-0.029722(4)	—	52758.0	52496–52994	35	1121
	1.82406350461(2)	-0.0297075(4)	-0.58(4)	53750.0	53007–54384	75	3667
	1.8240615852(2)	-0.02938(2)	—	54500.0	54463–54714	18	1118
B1758–23	2.40490661705(4)	-0.65316(2)	3(3)	52900.0	52494–53292	67	3079
	2.40484572830(1)	-0.6531075(6)	1.12(4)	54000.0	53327–54831	116	2604
B1800–21	7.48196609098(1)	-7.4862079(4)	238.57(3)	52800.0	51916–53429	165	7091
	7.481282565107(9)	-7.5200390(9)	207.93(4)	53900.0	53458–54832	108	12533
B1809–173	0.82961975150(3)	-0.013100(4)	—	52800.0	52529–53105	32	1360
	0.82961862949(2)	-0.0131283(4)	0.25(5)	53800.0	53119–54351	79	1013
	0.82961772349(6)	-0.01313(1)	—	54600.0	54382–54764	17	1214
B1815–14	3.43066049095(2)	-0.024011(3)	—	51822.0	51512–52048	69	558
	3.430655769877(4)	-0.0239594(2)	-0.446(3)	54100.0	52081–54831	226	2400
B1822–09	1.300387566396(6)	-0.0886064(2)	4.34(4)	53280.0	52811–53716	83	1362
	1.30038260224(2)	-0.088638(3)	-22.0(6)	53930.0	53723–54094	45	1203
	1.30038021608(2)	-0.088780(2)	-2.8(1)	54262.0	54129–54831	54	1543
B1823–13	9.85460718889(1)	-7.2729146(3)	105.74(2)	52400.0	51574–53199	132	3407
	9.85394781571(6)	-7.265061(9)	66(1)	53450.0	53254–53730	32	389
	9.85349875132(2)	-7.3062994(9)	280.88(9)	54200.0	53739–54518	90	14061
B1838–04	5.37205530549(3)	-0.184289(2)	1.5(2)	53044.0	52535–53387	57	364
	5.37204477631(1)	-0.1844913(5)	-1.56(4)	53900.0	53429–54662	99	556
J1853+0545	7.91137412600(2)	-0.038303(1)	—	53100.0	52493–53434	63	446
	7.91137154739(1)	-0.0383351(1)	-0.19(5)	53882.0	53458–54830	113	549
B1900+06	1.484775165625(2)	-0.01700231(8)	—	53390.0	52473–54240	129	340
	1.48477368242(2)	-0.017003(1)	—	54400.0	54262–54821	39	306
B1907+10	3.52558388053(5)	-0.03286(3)	—	52578.0	52470–52686	18	161
	3.525581831083(6)	-0.0328630(5)	—	53300.0	52705–53689	71	391
	3.52557928013(1)	-0.0328110(3)	-2.02(4)	54200.0	53701–54821	88	350
B1913+10	2.471906137401(5)	-0.0931843(1)	-0.071(9)	53308.0	52473–54159	118	311
	2.47189777002(2)	-0.093219(1)	—	54348.0	54180–54831	61	306
B2224+65	1.465111203809(5)	-0.0207375(4)	-0.268(9)	53880.0	52487–54265	220	922
	1.46511023680(2)	-0.020737(2)	—	54420.0	54275–54831	71	484

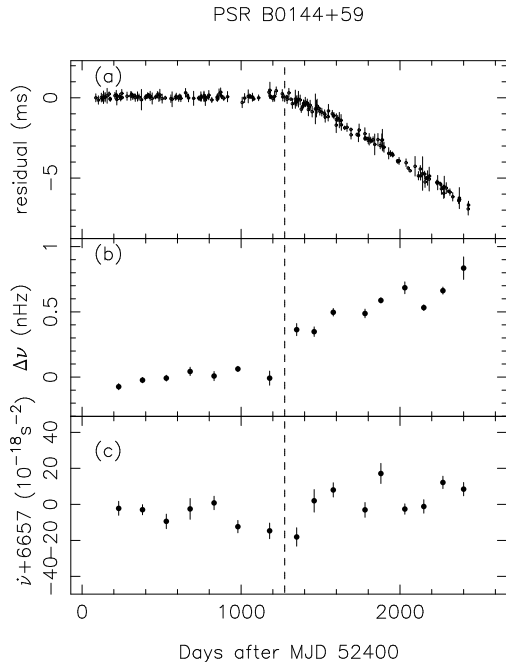


Figure 1. The 2005 December glitch of PSR B0144+59: (a) timing residuals relative to the pre-glitch model. (b) variations of the frequency residual $\Delta\nu$ relative to the pre-glitch solution. (c) the variations of $\dot{\nu}$. The dashed vertical line indicates the epoch of the glitch.

3.1 PSR B0144+59

This pulsar has a period of 196 ms and a small period derivative implying a relatively large characteristic age of 12.1 Myr. Normally it is a very stable pulsar and has no previously detected glitch. Despite this, we detected a very small glitch at MJD ~ 53682 , with a fractional frequency step of just 0.055×10^{-9} . There are only four measured glitches with fractional size smaller than this. Also, PSR B0144+59 is the second oldest pulsar for which a glitch has been observed, with the oldest being the millisecond pulsar PSR B1821–24 which has a characteristic age of 29.9 Myr. Fig. 1 shows that after the glitch there is continuous increase of the frequency relative to the extrapolated pre-glitch (i.e., positive $\Delta\dot{\nu}_p$ or decrease in $|\dot{\nu}|$) that lasts for at least 600 d. This is unusual and opposite to the normal post-glitch decay. It is possible that this tiny glitch in PSR B0144+59 is just a fluctuation in the timing noise, but it does appear distinct in the $\Delta\nu$ plot. Similar decreases in $|\dot{\nu}|$ following a glitch were observed for PSR B1951+32 (Foster et al. 1990) and in the RRAT PSR J1819–1458 (Lyne et al. 2009). These may imply an increase in the moment of inertia or a decrease in the spin-down torque at the time of the glitch. For the PSR B0144+59 position fit given in Table 1, whitening of the residuals required two frequency derivatives.

3.2 PSR B0402+61

This pulsar is also relatively old with $\tau_c \sim 1.7$ Myr. Fig. 2 shows a small glitch at MJD ~ 53041 (2004 February) with $\Delta\nu_g/\nu \sim 0.6 \times 10^{-9}$. In contrast to PSR B0144+59, there is an almost linear decrease of ν relative to the pre-glitch value that lasts for at least 1000 days and overshoots the pre-glitch

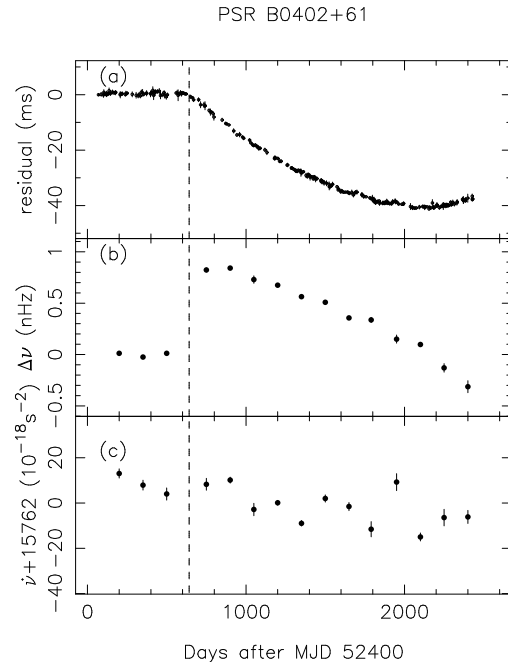


Figure 2. The glitch of PSR B0402+61: (a) timing residuals relative to the pre-glitch model, (b) variations of frequency residual $\Delta\nu$ relative to the pre-glitch solution, (c) the variations of $\dot{\nu}$.

extrapolation. This is similar to the behaviour seen in the Crab pulsar (Lyne et al. 1993). The negative $\Delta\dot{\nu}_p$ is seen in Fig. 2 (b) and is listed in Table 3.

3.3 PSR B0525+21

This very long-period pulsar has had three small glitches reported. The first at MJD 42057 (January 1974) had a magnitude of $\Delta\nu_g/\nu = 1.2 \times 10^{-9}$ and an exponential decay with $Q = 0.5$ and timescale 150 days was measured (Downs 1982; Shemar & Lyne 1996). Janssen & Stappers (2006) reported a second glitch of similar magnitude at MJD 52284 and suggest that a very small glitch with $\Delta\nu_g/\nu = 0.17 \times 10^{-9}$ may have occurred at MJD 53375. Our data, shown in Fig. 3, confirm the glitch at MJD 52284 (our central date is MJD 52280 but the dates are consistent within the uncertainties). The measured Q and τ_d values are similar to those for the 1974 glitch. Our data also show another small glitch of magnitude $\Delta\nu_g/\nu = 0.43 \times 10^{-9}$ at MJD 53980. However, Fig. 3 shows no evidence for the small glitch (of amplitude $\Delta\nu \sim 0.05$ nHz) at MJD 53375 claimed by Janssen & Stappers (2006). Although this epoch coincides with a small gap in our data, a limit of ~ 0.01 nHz can be placed on the amplitude of any glitch at this time. Since Janssen & Stappers (2006) did not show time or frequency residuals for this pulsar, it is not possible to comment on what led them to believe that there was a glitch at this time. We note that it is the smallest of the three glitches that they reported for this pulsar.

3.4 PSR J0631+1036

PSR J0631+1036, discovered by Zepka et al. (1996), has a period of 288 ms and a very large period derivative of $105 \times$

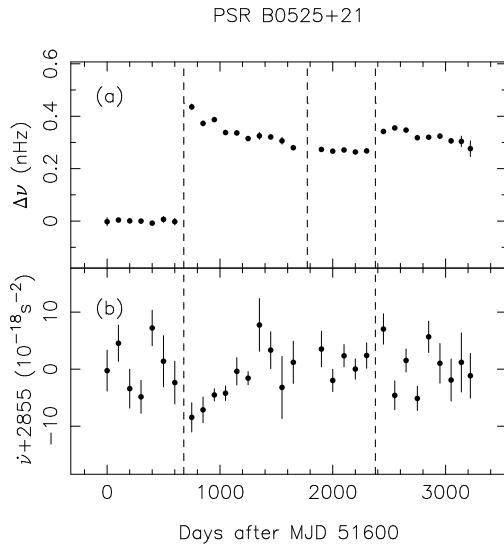


Figure 3. Glitches of PSR B0525+21: (a) variations of frequency residual $\Delta\nu$ relative to the pre-glitch solution, and (b) the frequency first derivative $\dot{\nu}$. The long dashed lines are at the epochs of well-defined glitches; the short dashed line is at the epoch of the small glitch claimed by Janssen & Stappers (2006).

10^{-15} implying a small characteristic age ~ 44 kyr. As shown in Fig. 4, three normal glitches and one unusual event which may be a slow glitch were detected in our data. The first glitch at MJD 52852 has an amplitude of $\Delta\nu_g/\nu \sim 19 \times 10^{-9}$ and shows a clear relaxation which is well described by an exponential decay model with $\tau_d \sim 120$ d and $Q \sim 0.62$ (Table 3). A small second glitch was detected around MJD ~ 53229 . Although it is not so obvious in Fig. 4, timing residuals around the time of the glitch given in Fig. 5 confirm its reality. Its relative magnitude is $\sim 1.6 \times 10^{-9}$.

Fig. 4 shows another event starting at MJD ~ 54129 which may be related to the slow glitches detected in PSR B1822–09 (Shabanova 1998; Zou et al. 2004; Shabanova 2007). At MJD ~ 54129 there is a sudden increase in $\dot{\nu}$ (decrease in $|\dot{\nu}|$) leading to a gradual increase in ν of ~ 23 nHz over about 130 d. During this time, $\dot{\nu}$ steadily decreased, over-shooting the pre-event value and returning ν to the extrapolation of its behaviour before the event. Table 3 lists the maximum $\Delta\nu_g/\nu$ of $\sim 6.6 \times 10^{-9}$. This behaviour is similar to that of the slow glitches observed in PSR B1822–09 (Shabanova 2007) except that the rise in $\dot{\nu}$ appears more abrupt and no overshoot is observed for PSR B1822–09, leading to a more permanent increase in ν relative to the pre-glitch solution.

A fourth glitch occurred in June 2008, with an amplitude of $\Delta\nu_g/\nu \sim 44 \times 10^{-9}$. Although the data span after this event is short, it can be seen from the Fig. 4 that there is a jump in $|\dot{\nu}| \sim 3 \times 10^{-15} \text{ s}^{-2}$ at the time of the glitch followed by some recovery. It is too early to say if the recovery is exponential, similar to that for the glitch at MJD 52852.

3.5 PSR J1705–3423

This pulsar, discovered in the Parkes Southern Pulsar Survey by Manchester et al. (1996), has a period of 0.255 s and period derivative of 1.07×10^{-15} . A small glitch was detected

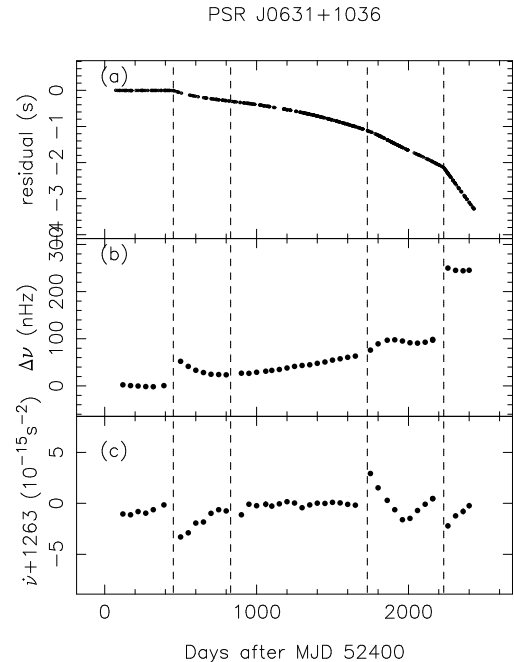


Figure 4. Glitches of PSR J0631+1036: (a) timing residuals relative to the pre-glitch model, (b) variations of frequency residual $\Delta\nu$ relative to the pre-glitch solution, and (c) the frequency first derivative $\dot{\nu}$.

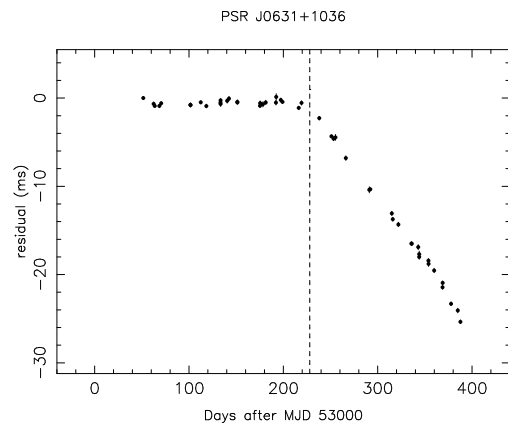


Figure 5. Timing residuals around the time of the small glitch in PSR J0631+1036.

in Oct 2007. A plot of the time variation of $\Delta\nu$ is given in Fig. 6a. The dominant effect is a small change in ν , with a magnitude of $\sim 2.0 \times 10^{-9}$ Hz. Fig. 6b shows no obvious change in $\dot{\nu}$.

3.6 PSR B1737–30

PSR B1737–30 is a young radio pulsar which has exhibited 20 glitches in 20 years, making it one of the most frequently glitching pulsars known (McKenna & Lyne 1990; Shemar & Lyne 1996; Krawczyk et al. 2003; Zou et al. 2008). The relative glitch amplitudes range widely from a few parts in 10^{-9} to nearly 2×10^{-6} . Significant increases in $|\dot{\nu}|$ at the time of the glitch are observed, at least for the larger glitches, and these tend to decay linearly with time.

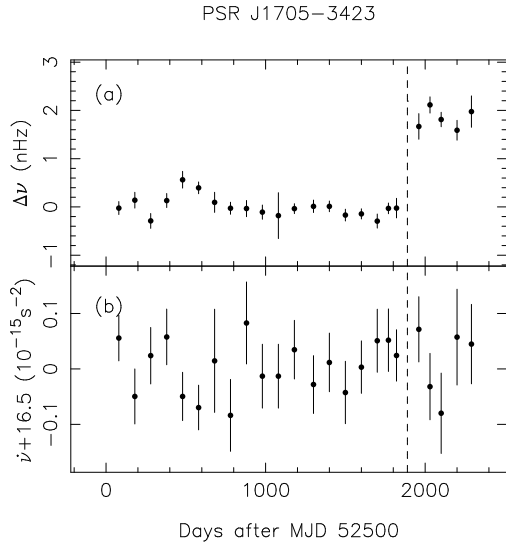


Figure 6. Timing behaviour of PSR B1705-3423: (a) variations of rotational frequency $\Delta\nu$ relative to the pre-glitch value, and (b) variations of the frequency first derivative $\dot{\nu}$.

Fig. 7 shows the last (giant) glitch observed by Zou et al. (2008) and two further smaller glitches at MJD ~ 54447 and ~ 54694 . Following the large glitch there is a short-term (~ 100 d) exponential recovery in $\dot{\nu}$ followed by an approximately linear increase in $\dot{\nu}$ until the next glitch. This behaviour is very similar to that observed in the Vela pulsar (Lyne et al. 1996) as will be discussed further in §4. Following this large glitch, no further glitches were observed for 1400 days, an unusually long “quiet” period for this pulsar. A small glitch with $\Delta\nu_g/\nu \sim 41 \times 10^{-9}$ was detected at MJD ~ 54447 . Then, about 280 d later, we observed another small glitch with $\Delta\nu_g/\nu \sim 2.4 \times 10^{-9}$. This brings the mean glitch rate back close to one per year.

3.7 PSR J1751-3323

This pulsar was discovered in a Parkes multi-beam survey by Kramer et al. (2003). In addition to its noisy timing behaviour, two small glitches were detected around MJD 53004 and 54435 with $\Delta\nu_g/\nu \sim 2 \times 10^{-9}$ and $\Delta\nu_g/\nu \sim 3 \times 10^{-9}$ respectively. Fig. 8 shows that no significant changes in $\dot{\nu}$ can be associated with these glitches.

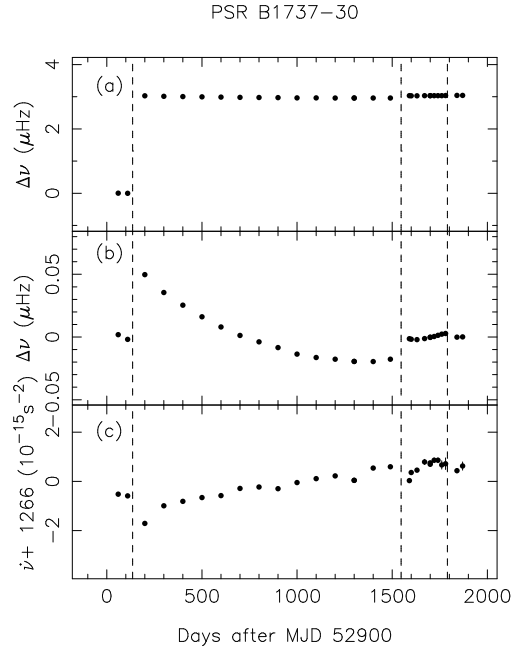


Figure 7. Glitches of PSR B1737-30: (a) variations of rotational frequency $\Delta\nu$ relative to the pre-glitch value, (b) an expanded plot of $\Delta\nu$ where the mean post-glitch value has been subtracted from the post-glitch data, and (c) variations of the frequency first derivative $\dot{\nu}$.

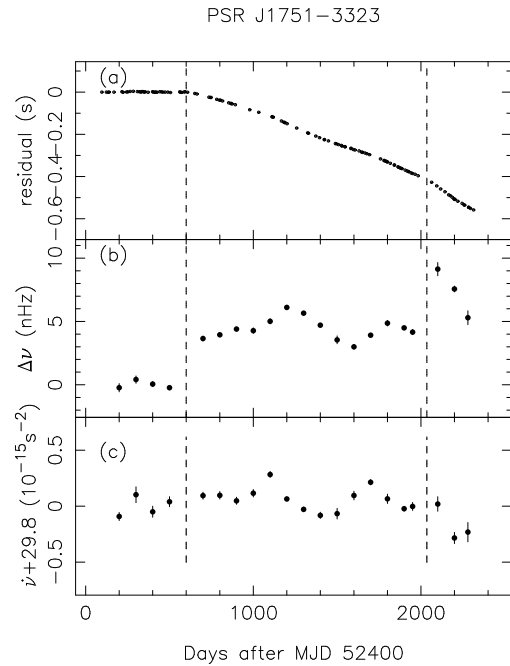


Figure 8. The glitches of PSR J1751-3323: (a) timing residuals, (b) frequency residuals $\Delta\nu$ relative to the pre-glitch solution, and (c) the variations of $\dot{\nu}$.

Table 3. The glitch parameters.

Pulsar Name	Epoch MJD	Extrapolated		Fitted					res (μ s)	Data Range
		$\Delta\nu_g/\nu$ (10^{-9})	$\Delta\dot{\nu}_g/\dot{\nu}$ (10^{-3})	$\Delta\nu_g/\nu$ (10^{-9})	$\Delta\dot{\nu}_g/\dot{\nu}$ (10^{-3})	$\Delta\dot{\nu}_p$ (10^{-15} s^{-2})	Q	τ_d (d)		
B0144+59	53682(15)*	0.056(3)	-0.21(5)	0.055(8)	-0.22(8)	0.0015(8)	-	-	128	52486-54831
B0402+61	53041(6)*	0.62(4)	0.5(1)	0.60(4)	0.47(16)	-0.007(2)	-	-	407	52469-54517
B0525+21	52280(4)*	1.53(5)	0.9(1)	1.6(2)	1.1(1)		0.44(5)	650(50)	620	51547-53975
	53980(12)*	0.5(1)	0.13(12)	0.43(6)	0.24(18)		-	-	769	53387-54517
J0631+1036	52852.0(2)*	17.6(9)	3.3(2)	19.1(6)	3.1(6)		0.62(5)	120(20)	518	52606-53143
	53229(10)	1.5(4)	-0.08(5)	1.6(7)	0.3(4)		-	-	249	53051-53387
	54129-54260	6.6(4)	-2.5(2)	-	-		-	-		
	54632.41(14)*	44(2)	5.7(5)	44(1)	4(2)		0.13(2)	40(15)	257	54437-54750
J1705-3423	54384(10)*	0.51(4)	-0.1(5)	0.52(5)	0.0(6)		-	-	660	52486-54832
B1737-30	54447.41(4)*	42(3)	0.2(4)	41.0(2)	0.7(1)		-	-	1811	53101-54696
	54694(3)*	2.2(4)	0.61(5)	2.4(3)	0.86(6)		-	-	299	54463-54807
J1751-3323	53004(6)*	2.3(3)	-1.4(6)	2.0(2)	-2.1(4)		-	-	883	52496-53433
	54435(8)*	3(1)	-1(3)	3.0(4)	1(3)		-	-	3683	53051-54620
B1758-23	53309(18)	493.2(4)	0.26(5)	494(1)	0.19(3)		0.009(2)	1000(100)	2896	52494-54606
B1800-21	53444(16)	3910(12)	8.69(8)	3914(2)	10.0(4)	-48(2)	0.009(1)	120(20)	618	53218-53778
B1809-173	53105(2)*	14.4(5)	3(1)	14.8(6)	3.6(5)		0.27(2)	800(100)	1080	52529-54394
	54367(13)*	1.5(3)	0.4(9)	1.6(4)	0.4(9)		-	-	1070	53450-54764
B1815-14	52057(7)	0.54(5)	-0.7(4)	0.54(4)	-0.8(4)		-	-	511	51510-52498
B1822-09	53719-53890	7.2(3)	-15.8(5)	-	-		-	-		
	54115.78(4)*	122(2)	-1.8(5)	121.3(2)	-1.9(3)		-	-	935	53742-54395
B1823-13	53238.2(7)*	3.4(3)	0.07(1)	3.5(3)	0.068(6)		-	-	584	52518-53730
	53734(5)	2416(4)	13.0(4)	2417(2)	14(5)	-44(9)	0.015(4)	75(25)	2668	53509-54080
B1838-04	53408(21)	578.7(4)	1.7(3)	578.8(1)	1.4(6)	-0.21(1)	0.00014(20)	80(20)	340	52536-54306
J1853+0545	53450(2)*	1.49(5)	1.6(5)	1.46(8)	3.5(7)		0.22(5)	250(30)	333	52494-54131
B1900+06	54248(11)*	0.33(3)	0.04(9)	0.33(3)	0.04(9)		-	-	334	52473-54821
B1907+10	52700(16)*	0.27(7)	0.5(7)	0.27(13)	0.5(10)		-	-	201	52470-53198
	53700-54400	1.52(5)	-5.0(7)	-	-		-	-		
B1913+10	54162(1)*	2.55(3)	0.08(5)	2.52(9)	0.3(1)		-	-	294	52473-54516
B2224+65	54266(14)*	0.36(8)	-0.8(4)	0.39(7)	-0.6(4)		-	-	417	53600-54706

* Glitch epoch determined by phase fit

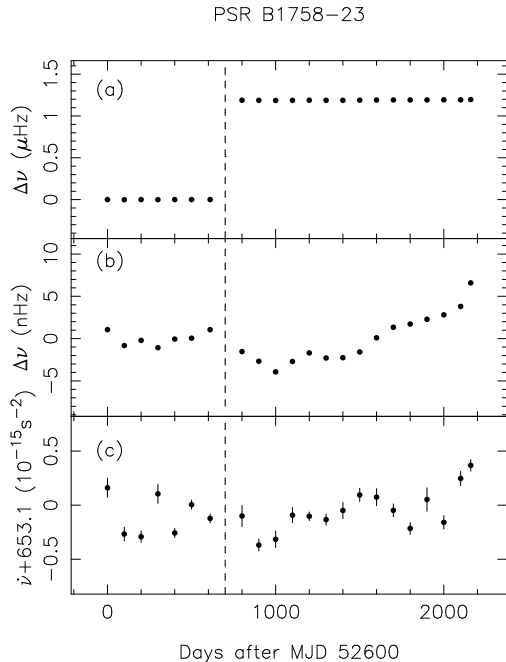


Figure 9. The glitch of PSR B1758–23: (a) variations of frequency residual $\Delta\nu$ relative to the pre-glitch solution, (b) an expanded plot of $\Delta\nu$ where the mean post-glitch value has been subtracted from the post-glitch data, and (c) the frequency first derivative $\dot{\nu}$.

3.8 PSR B1758–23

This pulsar has a period of 415 ms and large period derivative giving it a small characteristic age of 58 kyr. PSR B1758–23 is distant and has a large dispersion measure ($DM = 1074 \text{ cm}^{-3} \text{ pc}$), resulting in a scattered pulse profile at 1.4 GHz. Furthermore, the pulsar suffers frequent glitches, so it is difficult to obtain a position measurement from timing; the value quoted in Table 1 is from the VLA observations of Frail et al. (1993).

Six glitches in this pulsar have been reported (Kaspi et al. 1993; Shemar & Lyne 1996; Wang et al. 2000; Krawczyk et al. 2003), with $\Delta\nu_g/\nu$ in the range $(0.02 - 0.34) \times 10^{-6}$. Little or no change in $\dot{\nu}$ is observed, showing that glitches in this pulsar have no significant post-glitch recovery. Our observations (Fig. 9) reveal a further glitch with $\Delta\nu_g/\nu \sim 0.494 \times 10^{-6}$ at MJD ~ 53309 , the largest seen for this pulsar. As for previous glitches in this pulsar, there is little or no post glitch decay (Fig. 9b and c), with the fitted value of $Q \sim 0.009$.

3.9 PSR B1800–21

Two giant glitches were detected for PSR B1800–21 in 1990 and 1997 with $\Delta\nu_g/\nu \sim 10^{-6}$ (Shemar & Lyne 1996; Wang et al. 2000), while a small glitch with $\Delta\nu_g/\nu \sim 5 \times 10^{-9}$ in 1996 was found by Krawczyk et al. (2003). Another giant glitch was detected in 2005 March (MJD ~ 53444) in our observations. As shown in Fig. 10, the fractional jump in frequency is $\Delta\nu_g/\nu \sim 3.9 \times 10^{-6}$. There is an exponential recovery of a small part of the change in ν and $\dot{\nu}$ with a time constant of about 120 days, but the main observed recovery is linear. A similar linear increase in $\dot{\nu}$ following the

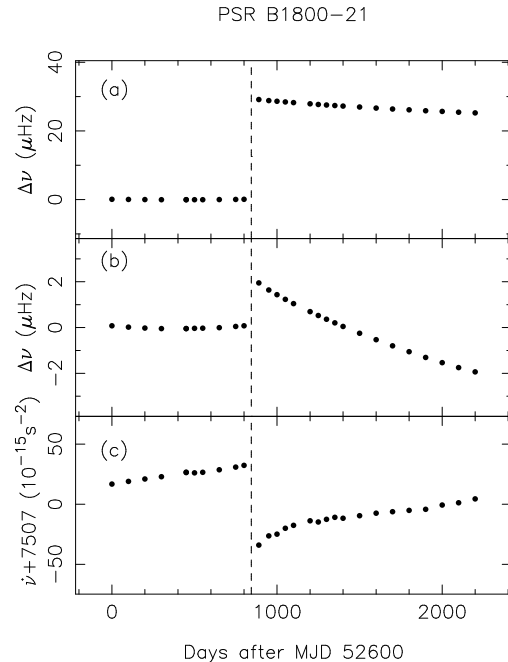


Figure 10. The glitch of PSR B1800–21: (a) variations of frequency residual $\Delta\nu$ relative to the pre-glitch solution, (b) an expanded plot of $\Delta\nu$ where the mean post-glitch value has been subtracted from the post-glitch data, and (c) the variations of $\dot{\nu}$.

previous jump can be seen in Fig. 10 (c). Once again, this is similar to the Vela pulsar post glitch behaviour (Lyne et al. 1996). Table 2 shows a large $\dot{\nu}$ both before and after the glitch corresponding to this linear recovery.

3.10 PSR B1809–173

PSR B1809–173 suffered a modest jump of fractional size $\Delta\nu_g/\nu \sim 14.3 \times 10^{-9}$ and $\Delta\dot{\nu}/\dot{\nu} \sim 3.3 \times 10^{-3}$ in 2004 April (MJD ~ 53105). Observed frequency variations are shown in Fig. 11. An exponential decay model with $\tau_d \sim 800$ d and $Q \sim 0.27$ is an adequate representation of the post-glitch relaxation. A second small glitch at Sep 2007 (MJD ~ 54367) with $\Delta\nu_g/\nu \sim 1.6 \times 10^{-9}$ is also detected.

3.11 PSR B1815–14

Fig. 12 shows that a small glitch was detected in PSR B1815–14 around MJD 52057. Fits of a second-order polynomial to the pre-glitch data and cubic polynomial to the post-glitch data are given in Table 2. Both these and the phase-coherent glitch fit are consistent with a glitch of magnitude $\Delta\nu_g/\nu \sim 0.54 \times 10^{-9}$ and $\Delta\dot{\nu}/\dot{\nu} \sim -0.8 \times 10^{-3}$. The post-glitch data show a quasi-periodic oscillation in residuals with period ~ 1200 d as illustrated in Fig. 13. Similar quasi-periodic oscillations in timing residuals have been observed in very long data spans by Hobbs et al. (2009). An increase in $\dot{\nu}$ (decrease in $|\dot{\nu}|$) was observed from MJD ~ 54000 lasting for ~ 200 d. This event, which is similar to the slow glitches observed in PSR B1822–09, results in an increase in ν , with $\Delta\nu \sim 5$ nHz. It is possible that similar but smaller fluctuations in $\dot{\nu}$ at earlier times result in the quasi-periodicity in ν and the timing residuals.

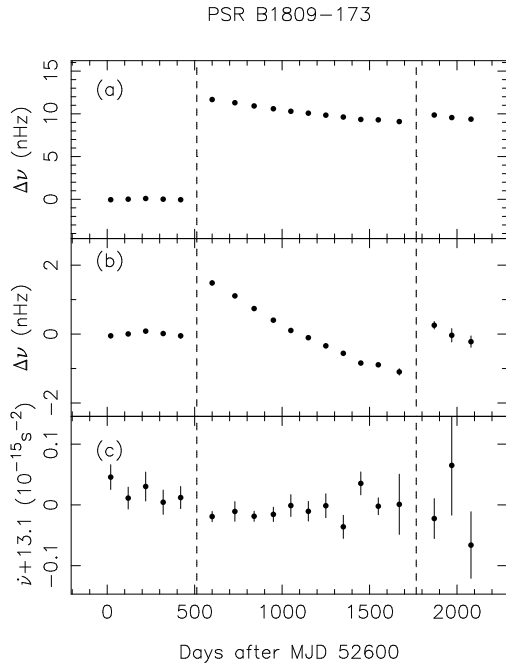


Figure 11. The glitches of PSR B1809–173: (a) variations of frequency residual $\Delta\nu$ relative to the pre-glitch solution, (b) an expanded plot of $\Delta\nu$ where the mean post-glitch value has been subtracted from the post-glitch data, and (c) the frequency first derivative $\dot{\nu}$.

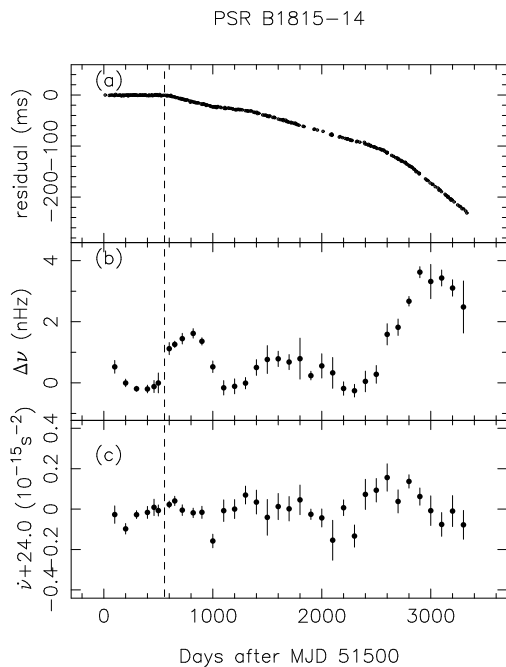


Figure 12. The glitch of PSR B1815–14: (a) timing residuals relative to the pre-glitch solution, (b) variations of frequency residual $\Delta\nu$ relative to the pre-glitch solution, and (c) the variations of $\dot{\nu}$.

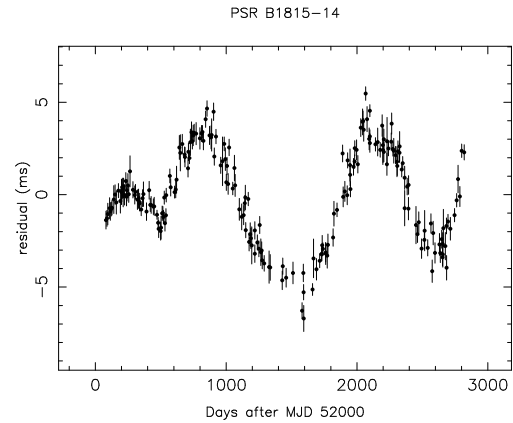


Figure 13. Timing residuals for PSR B1815–14 after the glitch with respect to the model given in Table 2.

3.12 PSR B1822–09

A total of seven glitches in PSR B1822–09 have been reported in the previous 12 years (Shabanova 1998; Zou et al. 2004; Shabanova 2007). Five of these glitches are “slow”, characterised by a relatively sharp rise in $\dot{\nu}$ followed by a decline to roughly its pre-glitch state over 100 – 200 d. This results in a gradual spin-up of the pulsar relative to its pre-glitch state to a new level at which it remains till the next event. A similar event was observed in PSR J0631+1036 as reported above in § 3.4. Here we extend the analysis of Zou et al. (2004) by another four years. Fig. 14 shows that a slow glitch started at MJD ~ 53720 and a “normal” glitch occurred at MJD ~ 54116 . The former was also seen by Shabanova (2007) around MJD 53740 near the end of her data set. The frequency first derivative $\dot{\nu}$ shows a sudden jump of $\sim 1.6 \times 10^{-15}$ at the start of the event. The spin frequency increases for about 200 d with respect to the pre-glitch fit until the increase in $\dot{\nu}$ decays away.

For the larger and latest glitch, $\Delta\nu_g/\nu \sim 0.121 \times 10^{-6}$. Probably because of timing noise and the short post-glitch data span, no clear post-glitch exponential recovery can be seen. Zou et al. (2004) suggested that a small-magnitude slow glitch probably occurred near the end of their data span around MJD 52900. Although there is a small fluctuation in ν and $\dot{\nu}$ visible in Fig. 14 at this time, we consider that it is not clear enough to be identified as a slow glitch.

3.13 PSR B1823–13

PSR B1823–13 is a young pulsar (~ 21.4 kyr) with a period of 101.4 ms. Two large glitches have been previously reported by Shemar & Lyne (1996) with $\Delta\nu_g/\nu \sim 2.7 \times 10^{-6}$ and $\Delta\nu_g/\nu \sim 3.0 \times 10^{-6}$ in 1986 and 1992 respectively. Both had a partial exponential recovery with timescale ~ 100 d followed by a linear increase in $\dot{\nu}$. As shown in Fig. 15, two new glitches were detected in the Nanshan timing. A small glitch with $\Delta\nu_g/\nu \sim 3.5 \times 10^{-9}$ occurred at MJD ~ 53238 , and a large glitch at MJD ~ 53734 with $\Delta\nu_g/\nu \sim 2.4 \times 10^{-6}$. There is no obvious relaxation after the small glitch, but after the large glitch the relaxation is very similar to that of the earlier large glitches in this pulsar. Fitting for a single exponential decay model with $\tau_d \sim 75$ d and $Q \sim 0.015$ gives a relatively good fit to the post-glitch data between MJD

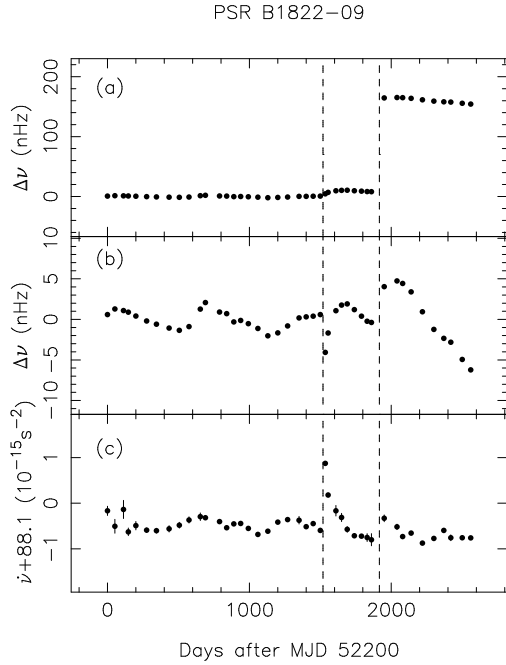


Figure 14. The glitches of PSR B1822–09: (a) variations of frequency residual $\Delta\nu$ relative to the pre-glitch solution, (b) an expanded plot of $\Delta\nu$ where the mean post-glitch value has been subtracted from the post-glitch data, and (c) the variations of $\dot{\nu}$.

53509 and 54080. Because of the small Q , there is effectively a permanent change in $\dot{\nu}$, $\Delta\dot{\nu}_p \sim -44 \times 10^{-15} \text{ s}^{-2}$. Fig. 15 shows a linear increase in $\dot{\nu}$ both before (through the small glitch) and after the larger glitch. Fitting to the linear part of the pre- and post-glitch data, despite the short data span after the glitch, we have $\ddot{\nu}$ approximately $100 \times 10^{-24} \text{ s}^{-3}$ and $65 \times 10^{-24} \text{ s}^{-3}$ respectively. We will further discuss this in §4.

3.14 PSR B1838–04

A large glitch with $\Delta\nu_g/\nu \sim 0.58 \times 10^{-6}$ was observed in PSR B1838–04 between MJD 53387 and 53429. This is the first glitch observed in this middle-aged pulsar which was discovered by Clifton & Lyne (1986). Fig. 16 shows a hint of a short exponential decay, but the main effect of the glitch is what seems to be a permanent change in $\dot{\nu}$. Fitting for this with a 80 d exponential decay gave a value of $\Delta\dot{\nu}_p$ of $-0.21 \times 10^{-15} \text{ s}^{-2}$ (Table 3).

3.15 PSR J1853+0545

We have detected the first known glitch for this recently discovered (Kramer et al. 2003) and relatively old pulsar (3.3 Myr). The glitch is small with a magnitude of $\Delta\nu_g/\nu \sim 1.46 \times 10^{-9}$. Fig. 17 shows a partial exponential recovery; fitting for this gives $\tau_d \sim 250 \text{ d}$, and fractional decay $Q \sim 0.22$.

3.16 PSR B1900+06

This pulsar has been monitored at Nanshan since 2002 and a small glitch was detected in May 2007 (MJD ~ 54248). The fractional size is $\Delta\nu_g/\nu \sim 0.33 \times 10^{-9}$. Fig. 18 shows

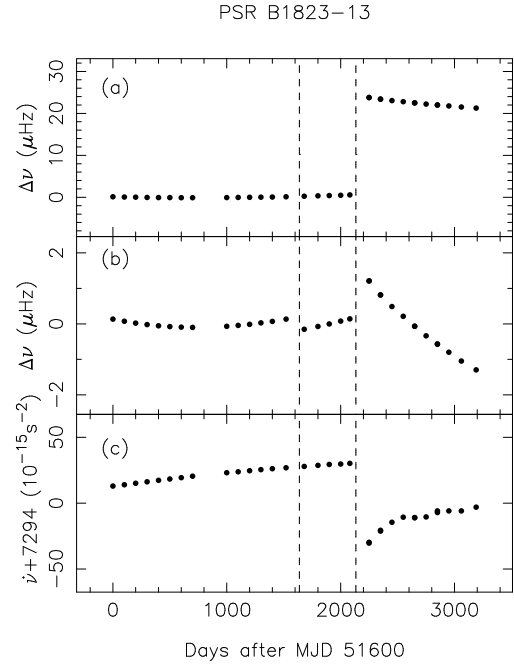


Figure 15. The glitches of PSR B1823–13: (a) variations of frequency residual $\Delta\nu$ relative to the pre-glitch solution, (b) an expanded plot of $\Delta\nu$ where the mean post-glitch value has been subtracted from the post-glitch data, and (c) the frequency first derivative $\dot{\nu}$.

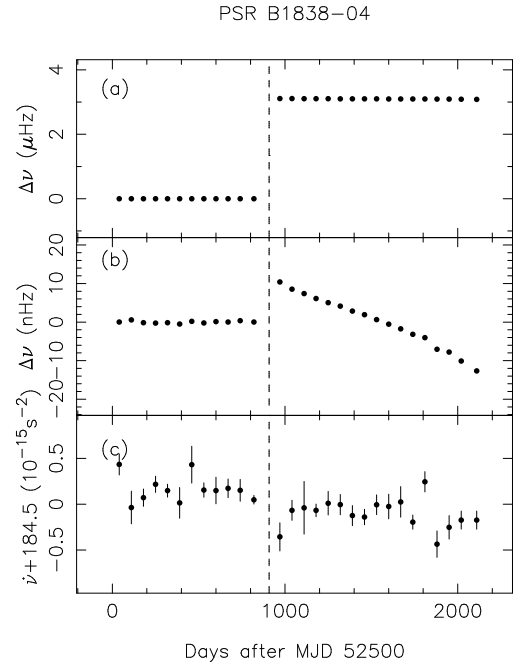


Figure 16. The glitch of PSR B1838–04: (a) variations of frequency residual $\Delta\nu$ relative to the pre-glitch solution, (b) an expanded plot of $\Delta\nu$ where the mean post-glitch value has been subtracted from the post-glitch data, and (c) the variations of $\dot{\nu}$.

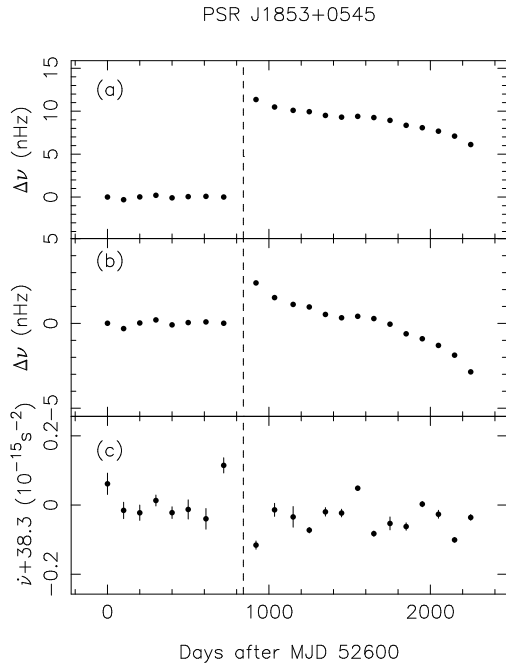


Figure 17. The glitch of PSR J1853+0545: (a) variations of frequency residual $\Delta\nu$ relative to the pre-glitch solution, (b) an expanded plot of $\Delta\nu$ where the mean post-glitch value has been subtracted from the post-glitch data, and (c) the variations of $\dot{\nu}$.

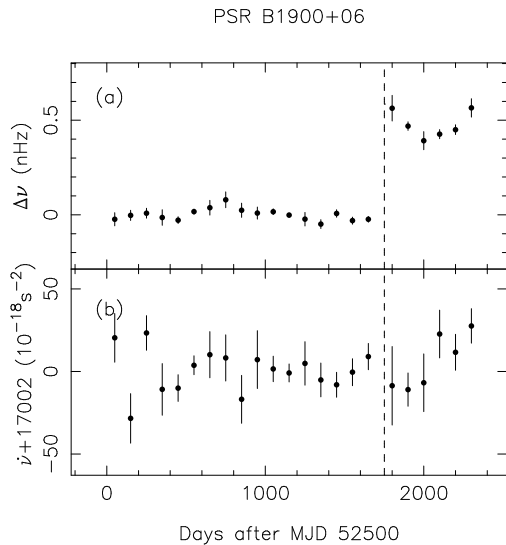


Figure 18. The glitch of PSR B1900+06: (a) variations of frequency residual $\Delta\nu$ relative to the pre-glitch solution, (b) the frequency first derivative $\dot{\nu}$.

that there may be some post-glitch recovery, but the data span is too short for further analysis.

3.17 PSR B1907+10

PSR B1907+10 has a period of 284 ms and is relatively old ($\tau_c \sim 1.7$ Myr). Fig. 19 shows a tiny glitch at MJD ~ 52700 with $\Delta\nu_g/\nu \sim 0.27 \times 10^{-9}$. Following that, there is evidence for a slow glitch between MJD ~ 53700 and ~ 54400 . A

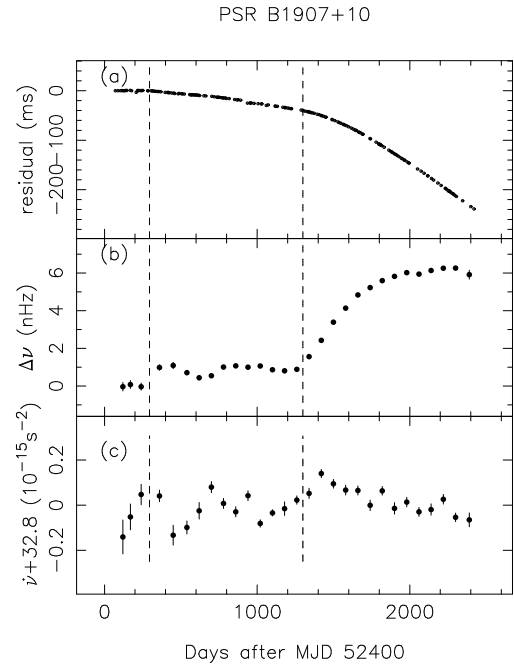


Figure 19. The glitches of PSR B1907+10: (a) timing residuals relative to the pre-glitch solution, (b) frequency residual $\Delta\nu$ relative to the pre-glitch solution, and (c) the variations of $\dot{\nu}$.

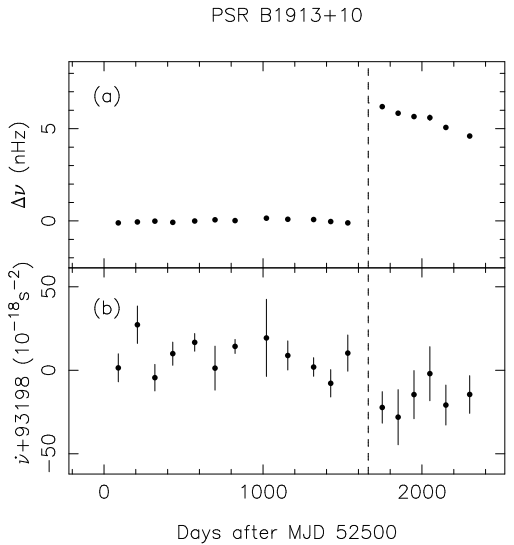


Figure 20. The glitch of PSR B1913+10: variations of (a) frequency residual $\Delta\nu$ relative to the pre-glitch solution, (b) the frequency first derivative $\dot{\nu}$.

gradual but significant increase in frequency of about 5 nHz was observed with a corresponding perturbation in $\dot{\nu}$. Although this may be just a fluctuation in the timing noise, it does have the characteristics of the slow jumps observed in PSR B1822–09 and some other pulsars.

3.18 PSR B1913+10

This pulsar has a period of 405 ms and characteristic age $\tau_c \sim 0.4$ Myr. Fig. 20 shows that a small glitch with $\Delta\nu_g/\nu \sim$

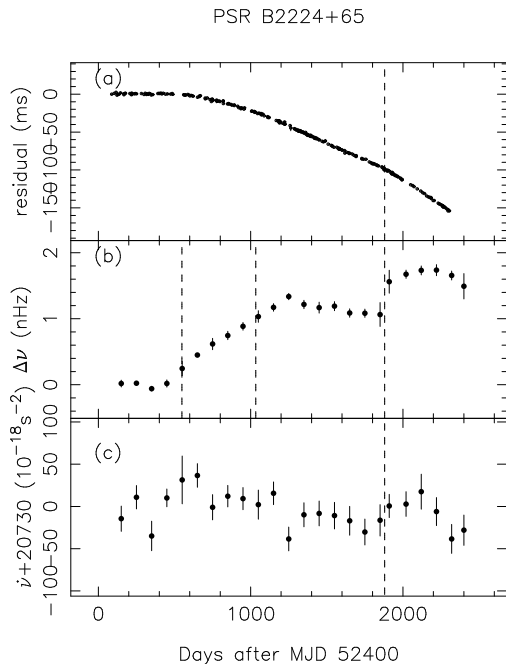


Figure 21. Glitches of PSR B2224+65: (a) timing residuals relative to pre-glitch model, (b) variations of frequency residual $\Delta\nu$ relative to the pre-glitch solution, and (c) the variations of $\dot{\nu}$. The short dashed lines in the $\Delta\nu$ plot mark the small glitches claimed by Janssen & Stappers (2006) and the longer dashed line marks the glitch detected in our data.

2.5×10^{-9} was observed at MJD ~ 54162 . Although the post-glitch data span is small, there is clear evidence for an increase in $|\dot{\nu}|$ indicating some post-glitch recovery.

3.19 PSR B2224+65

PSR B2224+65 is the high-velocity pulsar associated with the Guitar Nebula (Cordes et al. 1993). It has a period of 0.682 s and a characteristic age of 1.1 Myr. A giant glitch with $\Delta\nu_g/\nu \sim 1.7 \times 10^{-6}$ occurred in 1976 October (Backus et al. 1982) and three tiny glitches ($\Delta\nu_g/\nu < 0.2 \times 10^{-9}$) between 2000 December and 2005 March were reported by Janssen & Stappers (2006). The long dashed line in Fig. 21 marks another glitch detected in the Nanshan data. This event at MJD ~ 54266 has $\Delta\nu_g/\nu \sim 0.39 \times 10^{-9}$. There is some evidence that $|\dot{\nu}|$ decreased after the glitch, similar to PSR B0144+59 (§ 3.1).

The short dashed lines mark the second and third small glitches claimed by Janssen & Stappers (2006) at MJD 52950 and 53434 for which the estimated $\Delta\nu_g$ values were 0.12×10^{-9} Hz and 0.28×10^{-9} Hz, respectively. (Nanshan observations commenced in 2002 August, after the time of the first small glitch.) Fig. 21(b) shows that the pulse frequency was increasing (relative to the pre-glitch solution) across the interval covered by these claimed glitches, but the increase appears smooth and no glitch larger than about 0.1×10^{-9} Hz is evident in the data. As for PSR B0525+21, Janssen & Stappers (2006) did not give phase or frequency residual plots for this pulsar, so it is not possible to assess the evidence for their claimed glitches.

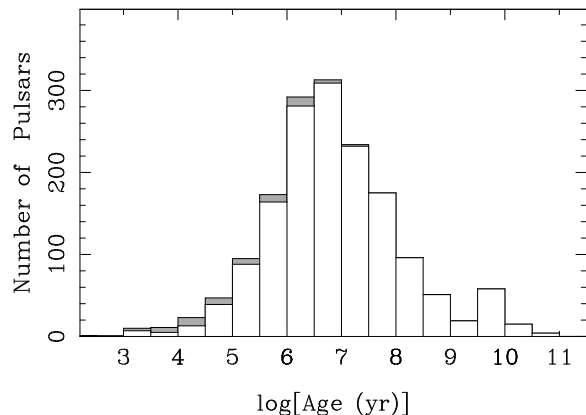


Figure 22. Distribution of known pulsars versus pulsar characteristic age with the distribution of glitching pulsars marked by the shaded area.

4 DISCUSSION

The study of pulsar glitches provides one of the few ways of probing the interior of neutron stars. Previous studies have shown that glitch properties, specifically characteristics of the post-glitch recovery, vary greatly from one pulsar to another and for different glitches in the same pulsar. Furthermore, while inter-glitch intervals are relatively short ($\lesssim 1$ yr) in some young pulsars, they are much longer in older pulsars, with many having no observed glitch over observing spans of 30 years or more. It is therefore valuable to continue timing observations of a large sample of pulsars in order to better characterise glitch properties and hopefully to lead to a better understanding of the mechanisms involved and the underlying properties of neutron stars.

This paper reports on glitches detected in continuing observations of a sample of 280 pulsars using the 25-m Nanshan telescope of Urumqi Observatory. We detected 29 glitches in 19 pulsars, with this being the first detection of a glitch in 12 of these pulsars. With those already listed in the ATNF Pulsar Catalogue, this increases the number of pulsars with detected glitches to 63 and the total number of detected glitches to 199. Fig. 22 shows the distribution of glitching pulsars among all known pulsars as a function of characteristic age. About half of all known pulsars with ages less than 3×10^4 yr have detected glitches, but for older pulsars the fraction is much less, with no glitches being detected in pulsars older than 3×10^7 yr.

The range of fractional glitch amplitude $\Delta\nu_g/\nu$ for glitches detected in our work is from 4.4×10^{-11} to 3.9×10^{-6} . Fig. 23 shows the distribution of fractional glitch amplitude for all known glitches³. The detection threshold for a glitch depends upon the quality of the TOAs, the frequency of the observations and the intrinsic timing noise. TOA uncertainties depend on the telescope and receiver parameters and the pulsar flux density and pulse width. For the Nanshan observations, they are typically 100 – 300 μ s. The pulsar timing project at Nanshan benefits from frequent and regular observations on a large sample of pulsars. Although there are

³ The three small glitches claimed by Janssen & Stappers (2006) for which we see no evidence have been omitted from this and subsequent figures.

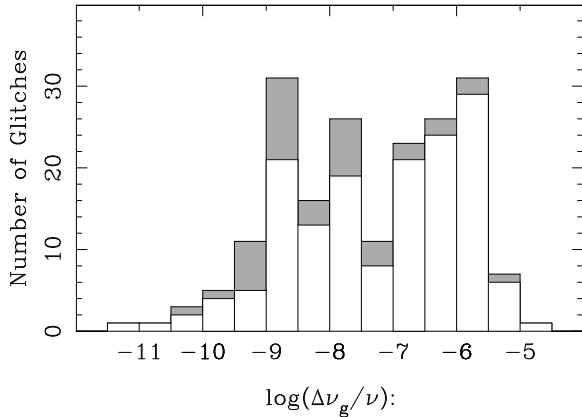


Figure 23. Distribution of relative glitch amplitudes of all known glitches. Those detected at Urumqi Observatory are marked by the shaded area.

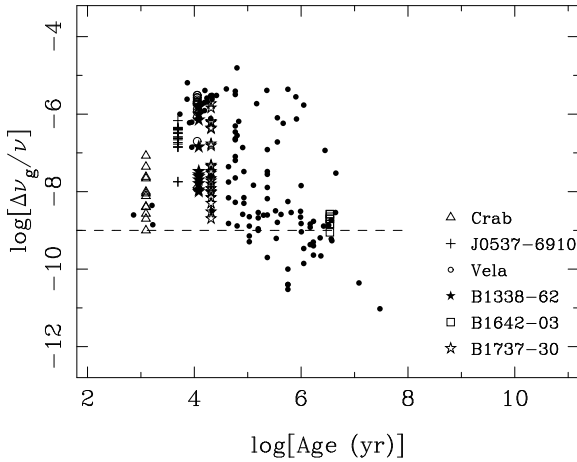


Figure 24. Fractional glitch amplitude $\Delta\nu_g/\nu$ versus characteristic age. The dash line marks the amplitude of $\Delta\nu_g/\nu = 10^{-9}$.

some longer gaps due to instrumental or scheduling issues, observations of all pulsars are typically at 10-day intervals. The level of intrinsic quasi-continuous timing noise varies greatly from pulsar to pulsar. This and the overall sensitivity of the observations to small glitches is best assessed from the $\Delta\nu$ plots given for each pulsar. Typically, the sensitivity is in the range $(0.1 - 1.0) \times 10^{-9}$ Hz. Our work has revealed eight small glitches with relative size $< 10^{-9}$. These studies have extended the sample of small glitches and indicate that the frequency of occurrence of small glitches is comparable to that of “giant” glitches with $\Delta\nu_g/\nu \gtrsim 10^{-6}$ (cf., Lyne et al. 2000).

Fig. 24 shows glitch fractional amplitudes plotted against the pulsar age. Although there is large scatter, there is a clear tendency for the average $\Delta\nu_g/\nu$ to increase with age up to somewhere between 10^4 and 10^5 years and then to decrease with increasing age. The increased detection of small glitches reported in this and other recent papers (Krawczyk et al. 2003; Cognard & Backer 2004; Janssen & Stappers 2006) has clarified this trend. Very small glitches with $\Delta\nu_g/\nu < 10^{-9}$ are only seen in pulsars with age greater than 10^5 yr.

Lyne et al. (2000) found that the jump in $\dot{\nu}$ at the time

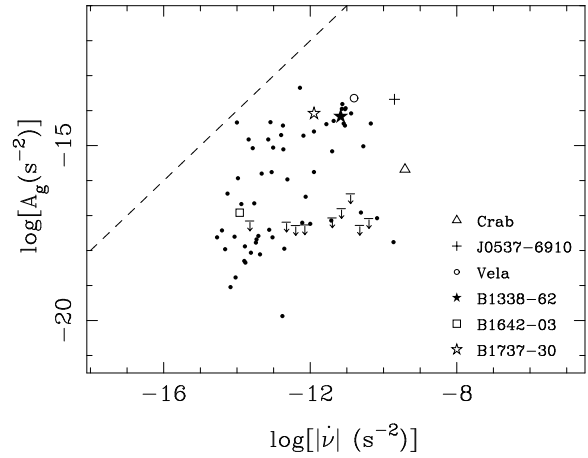


Figure 25. Plot of glitch activity parameter, A_g versus the absolute value of the spin-down rate $\dot{\nu}$. The dash indicates equal values of these two quantities. Upper limits of A_g are given by assuming one glitch $\Delta\nu_g/\nu = 10^{-9}$ occurred for young pulsars with no detected glitch and $\tau_c < 10^5$ yr. Frequent glitching pulsars are marked specifically.

of a glitch, $\Delta\dot{\nu}_g$, was related to the value of $\dot{\nu}$, with the fractional change $\Delta\dot{\nu}_g/\dot{\nu}$ being approximately constant. Table 3 shows that most of the measured values are about 10^{-3} , but there is a scatter of up to two orders of magnitude in the ratio, even for different glitches in a given pulsar.

The glitch activity parameter, A_g (Equation 1) is a way of quantifying the contribution of glitches to $\dot{\nu}$. Since pulsars slow down, $\dot{\nu}$ is negative, but glitches are spin-ups and hence the contribution is positive. In some models, the fractional contribution is related to the fraction of the neutron-star moment of inertia which is in superfluid form (e.g., Ruderman et al. 1998). Fig. 25 shows the dependence of activity parameter on $|\dot{\nu}|$. Again there is a large scatter, but there is a tendency for increasing activity with increasing $|\dot{\nu}|$ with the ratio between them ranging between 10^{-2} and 10^{-5} . There seems to be a turn-over for the pulsars with largest $|\dot{\nu}|$, for example the Crab pulsar and PSR J0537–6910, having relatively smaller activity parameters. There is one pulsar, PSR J2301+5852 (the 7 s anomalous X-ray pulsar 1E 2259+586 in the supernova remnant CTB 109), where this ratio is close to 1.0. However, it should be noted that only one glitch has been observed in this pulsar (Kaspi et al. 2003), so the derived activity parameter is effectively an upper limit.

Glitches are generally attributed to the release of stress built up as a result of the steady spin-down of the pulsar. This stress may be in the solid crust, relieved by crustal starquakes (Baym et al. 1969), or may be on pinned vortices in the superfluid interior, relieved by a collective unpinning of many vortices (Anderson & Itoh 1975). Both of these result in a sudden spin-up of the crust and hence a jump in the observed pulse frequency. In these models, one might expect a correlation of glitch size with the duration of the preceding or following inter-glitch interval, depending on the detailed mechanism. A strong correlation between the size of glitches and the length of the following inter-glitch interval was observed for PSRs J0537–6910 (Middlethick et al. 2006) and B1642–03 (Shabanova 2009), but such a clear correlation is not observed in other pulsars.

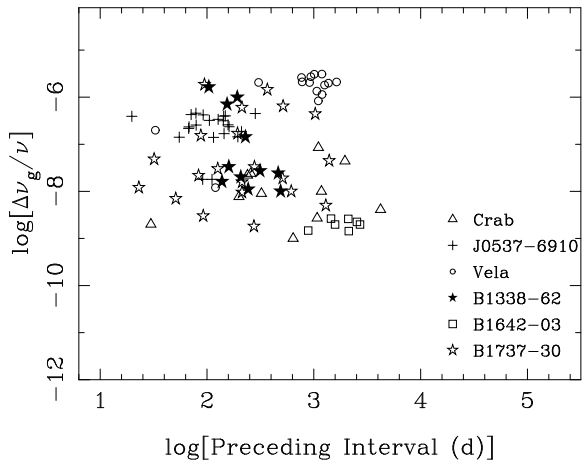


Figure 26. Fractional glitch amplitude versus length of the preceding interglitch interval.

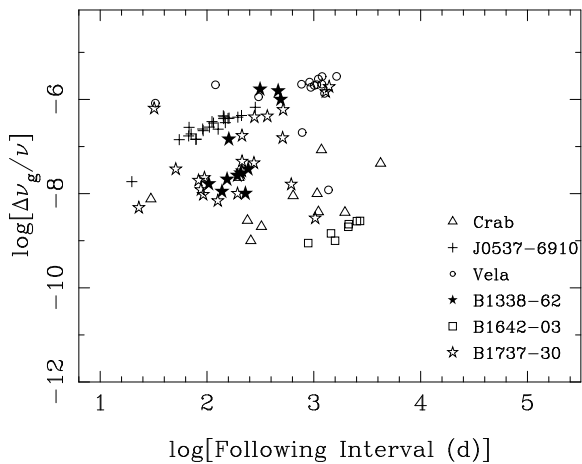


Figure 27. Fractional glitch amplitude versus length of the following interglitch interval.

Fig. 26 and 27 shows the dependence of the fractional glitch amplitude on the length of the preceding and following interglitch intervals respectively for the most frequently glitching pulsars. Despite the naive expectation that glitches would be large after a long build-up period, there is very little correlation of glitch amplitude with length of the preceding interval. For example, the Crab pulsar and PSR B1737-30 have a wide range of both parameters and there is essentially no correlation. Most glitches in the Vela pulsar are large and have long inter-glitch intervals. Two smaller glitches have been observed with shorter preceding intervals, but the preceding interval for the smallest glitch is more than four times the interval for the next smallest which is more than an order of magnitude larger. For PSR J0537-6910, there is no correlation and, for PSR B1338-62, if anything there is a negative correlation. For post-glitch intervals, Fig. 27 shows the correlations found by Middleditch et al. (2006) and Shabanova (2009) for PSR J0537-6910 and PSR B1642-03 respectively, and a possible steeper positive dependence for PSR B1338-62. Again for the Crab and Vela pulsars and PSR B1737-30 there is little correlation.

Pulsars have a wide variety of post-glitch behaviours. Most show some form of relaxation toward the extrapolated pre-glitch solution after a glitch. However, there are some cases where the pulsar simply keeps spinning at the new rate with no change in $\dot{\nu}$. In terms of the exponential decay model (Equations 3 – 7), $\Delta\nu_d \approx 0$, $\Delta\nu_g \approx \Delta\nu_p$, $Q \approx 0$ and $\Delta\dot{\nu}_g \approx 0$. PSR B1758-23 is a good example of a pulsar with large glitches having these characteristics. For small glitches, it is generally not possible to measure any decay since it is masked by random and systematic timing noise.

In some pulsars there is an apparently permanent change in $\dot{\nu}$ at the time of a glitch, for example, PSRs B0144+59, B0402+61, B1838-04 and B2224+65. For PSR B0144+59 and possibly PSR B2224+65, the change is positive which is unusual and not in accord with the exponential decay model. For the others, it is of course possible that the decay is exponential but with a time constant much longer than our post-glitch data span.

Exponential recoveries are seen in many pulsars, but these generally have relatively short timescales, ~ 100 d, and low Q , that is, only a fraction of the initial frequency jump decays. Examples are the first observed glitch in PSR J0631+1036 and the large glitches in PSRs B1800-21 and B1823-13. For PSR B1838-04, there is a short exponential recovery preceding the long-term decay mentioned above.

These small exponential recoveries are often associated with other post-glitch behaviours. For example, they precede linear increases in $\dot{\nu}$ in PSRs B1737-30, B1800-21 and B1823-13. The latter two pulsars also show an effectively permanent increase in $|\dot{\nu}|$ at the time of the glitch, that is, the linear post-glitch recovery is approximately parallel to but below that existing before the observed glitch (see Figures 10 and 15). Very similar behaviour is observed in the Vela pulsar (Lyne et al. 1996), and in PSRs B1046-58, B1706-44 and B1727-33 (Shemar & Lyne 1996; Wang et al. 2000). Table 4 gives the observed $\dot{\nu}$ slopes, i.e., $\ddot{\nu}$, for the linear portion of the recovery. The slope in the Vela pulsar is an order of magnitude greater than for the other pulsars. For PSRs B1800-21 and B1823-13, multiple glitches with linear behaviour are observed, but the slopes are distinctly different for the different glitches, varying by about a factor of two. Similar slope variations are evident in the Vela data (Lyne et al. 1996). The apparent braking indices

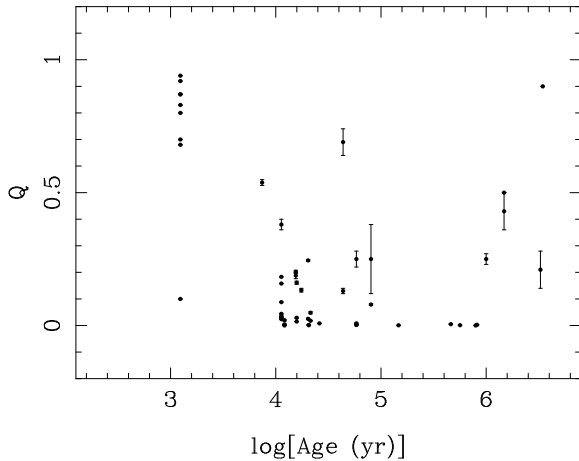
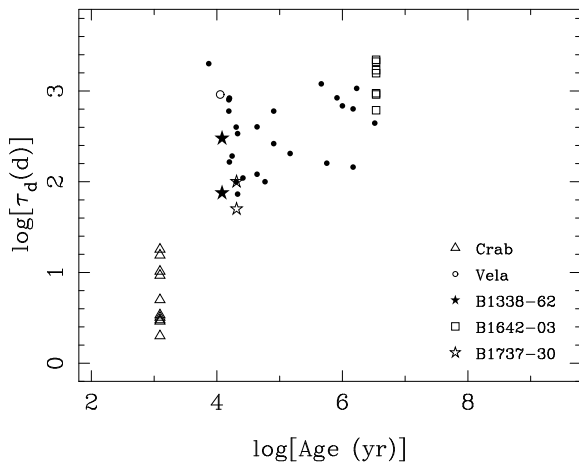
$$n = \frac{\ddot{\nu}\nu}{\dot{\nu}^2} \quad (8)$$

corresponding to the linear increases in $\dot{\nu}$ are also given in Table 4. Values range between 12 and 40, emphasising that these changes are due to internal dynamics in the neutron star, not to magnetic-dipole braking (for which $n = 3$). Although the Vela pulsar has the largest values, there is no clear correlation of either the slope or the braking index with pulse period or characteristic age. Table 4 also gives the maximum observed fractional glitch size, showing that all of these pulsars have giant glitches. However, it is worth noting that linear recoveries are not observed in PSRs B1338-62, J1617-5055, B1757-24 and J2021+3651, despite these having similar characteristic ages and similar maximum glitch sizes.

Fig. 28 shows the fraction of $\Delta\nu_g$ which decays, Q , versus characteristic age. Except for one event with $Q \sim 0.1$, the

Table 4. Rate of change of $\dot{\nu}$ for pulsars which show a linear post-glitch recovery.

Pulsar Name	P (s)	Age (kyr)	Max $\Delta\nu_g/\nu$ (10^{-6})	$\dot{\nu}$ (10^{-24} s^{-3})	n	Note
B0833–45	0.089	11.3	3.06(7)	873(10)	40.3(5)	MJD 50024–50364 (Wang et al. 2000)
B1046–58	0.124	20.3	2.995(7)	72(10)	15(2)	MJD 47909–48929 (Wang et al. 2000)
B1706–44	0.102	17.5	2.057(2)	124(1)	15.42(1)	MJD 47909–48746 (Wang et al. 2000)
B1727–33	0.139	26	3.033(8)	100.5(13)	37.6(5)	MJD 48100–49500 (Shemar & Lyne 1996)
B1737–30	0.606	20.6	1.8536(14)	12.69(1)	13.07(1)	MJD 53250–54394 (this work)
B1800–21	0.133	15.8	4.073(16)	236.5(1)	31.77(1)	MJD 51916–53429 (this work)
				188.1(1)	24.89(1)	MJD 53660–54832 (this work)
				107(30)	14(4)	MJD 46600–48425 (Shemar & Lyne 1996)
B1823–13	0.101	21.4	3.05(5)	106.3(5)	19.74(1)	MJD 51574–53199 (this work)
				65(2)	12.3(2)	MJD 53253–53723 (this work)
				203.0(1)	37.53(4)	MJD 53950–54832 (this work)

**Figure 28.** The fraction parameter Q in which a glitch $\Delta\nu_g$ decays, versus characteristic age.**Figure 29.** Glitch decay time-scale versus pulsar characteristic age.

Crab pulsar usually has a large Q between 0.7 and 1.0. Although there is some tendency for decreasing Q with increasing age (Wang et al. 2000), several old pulsars, for example, PSRs B0525+21, B1642–03, B1809–173 and J1853+0545 show some evidence for exponential relaxation. Fig. 29 shows that, with the addition of PSR B1642–03 (Shabanova 2009), there is a clearer correlation of decay timescale with age than was previously evident (Wang et al. 2000). This suggests a connection with the internal temperature of the neutron star (cf. Alpar et al. 1989).

Two new examples of the “slow glitch” phenomenon, in PSRs J0631+1036, and B1907+10, have been identified in this paper. Previously, slow glitches have only been identified in one pulsar, PSR B1822–09 (Shabanova 1998; Shabanova & Urama 2000; Zou et al. 2004; Shabanova 2005, 2007). Although it is possible to interpret these events as fluctuations in timing noise, they appear to be distinct and repeatable with similar characteristics. Hence it is reasonable to consider them as a separate category. PSR B1822–09 has had five slow glitches between 1995 and 2004 and one more in 2006 reported in this work. The new slow glitches detected in PSRs J0631+1036 and B1907+10 significantly increase the sample of slow glitches. The event in PSR J0631+1036 is similar in size and characteristics to those in PSR B1822–09, with an increment in $\dot{\nu}$ of about $2 \times 10^{-15} \text{ s}^{-2}$ lasting ~ 100 d. However it differs in that the decline in $\dot{\nu}$ overshoot the pre-event value, resulting in an effective spin-down of the period to approximately its extrapolated value. In PSR B1822–09, the spin-ups persist until the next event.

The results presented in this paper significantly increase the sample of known pulsar glitches. They further illustrate the complex nature of glitches, with a great diversity of glitch sizes and modes of post-glitch recovery being observed, both in individual pulsars and across different pulsars. They also strengthen the identification of slow glitches as a distinct phenomenon. While there are several different models for glitches, as yet none of these models satisfactorily account for this diversity and so the promise that glitches

have as probes of the interior of neutron stars has not yet been fully realised. Hopefully, these and future results will act as a stimulus for a better understanding of the mechanisms involved and their implications for the physics of neutron-star interiors.

ACKNOWLEDGMENTS

This work was supported by the Knowledge Innovation Program of CAS, Grant No. KJCX2-YW-T09, NSFC project No. 10673021, and National Basic Research Program of China (973 program 2009CB824800).

REFERENCES

- Alpar M. A., Cheng K. S., Pines D., 1989, *ApJ*, 346, 823
 Anderson P. W., Itoh N., 1975, *Nature*, 256, 25
 Backus P. R., Taylor J. H., Damashek M., 1982, *ApJ*, 255, L63
 Baym G., Pethick C., Pines D., 1969, *Nature*, 224, 673
 Baym G., Pethick C., Pines D., Ruderman M., 1969, *Nature*, 224, 872
 Brisken W. F., Carrillo-Barragan M., Kurtz S., 2006, *ApJ*, 652, 554
 Clifton T. R., Lyne A. G., 1986, *Nature*, 320, 43
 Cognard I., Backer D. C., 2004, *ApJ*, 612, L125
 Cordes J. M., Downs G. S., 1985, *ApJS*, 59, 343
 Cordes J. M., Romani R. W., Lundgren S. C., 1993, *Nature*, 362, 133
 Dodson R., Lewis D., McCulloch P., 2007, *Ap&SS*, 308, 585
 Downs G. S., 1982, *ApJ*, 257, L67
 Fomalont E. B., Goss W. M., Manchester R. N., Lyne A. G., 1997, *MNRAS*, 286, 81
 Foster R. S., Backer D. C., Wolszczan A., 1990, *ApJ*, 356, 243
 Frail D. A., Kulkarni S. R., Vasisht G., 1993, *Nature*, 365, 136
 Hobbs G., Faulkner A., Stairs I. H., Camilo F., Manchester R. N., Lyne A. G., Kramer M., D'Amico N., Kaspi V. M., Possenti A., McLaughlin M. A., Lorimer D. R., Burgay M., Joshi B. C., Crawford F., 2004, *MNRAS*, 352, 1439
 Hobbs G., Lyne A. G., Kramer M., 2009, *MNRAS*, in press
 Janssen G. H., Stappers B. W., 2006, *A&A*, 457, 611
 Kaspi V. M., Gavriil F. P., Woods P. M., Jensen J. B., Roberts M. S. E., Chakrabarty D., 2003, *ApJ*, 588, L93
 Kaspi V. M., Lyne A. G., Manchester R. N., Johnston S., D'Amico N., Shemar S. L., 1993, *ApJ*, 409, L57
 Kramer M., Bell J. F., Manchester R. N., Lyne A. G., Camilo F., Stairs I. H., D'Amico N., Kaspi V. M., Hobbs G., Morris D. J., Crawford F., Possenti A., Joshi B. C., McLaughlin M. A., Lorimer D. R., Faulkner A. J., 2003, *MNRAS*, 342, 1299
 Krawczyk A., Lyne A. G., Gil J. A., Joshi B. C., 2003, *MNRAS*, 340, 1087
 Lyne A. G., McLaughlin M. A., Keane E. F., Kramer M., Espinoza C. M., Stappers B. W., Palliyaguru N. T., Miller J., . 2009, *ArXiv e-prints*
 Lyne A. G., Pritchard R. S., Graham-Smith F., Camilo F., 1996, *Nature*, 381, 497
 Lyne A. G., Pritchard R. S., Smith F. G., 1993, *MNRAS*, 265, 1003
 Lyne A. G., Shemar S. L., Graham-Smith F., 2000, *MNRAS*, 315, 534
 McKenna J., Lyne A. G., 1990, *Nature*, 343, 349
 Manchester R. N., Hobbs G. B., Teoh A., Hobbs M., 2005, *AJ*, 129, 1993
 Manchester R. N., Lyne A. G., D'Amico N., Bailes M., Johnston S., Lorimer D. R., Harrison P. A., Nicastro L., Bell J. F., 1996, *MNRAS*, 279, 1235
 Middleditch J., Marshall F. E., Wang Q. D., Gotthelf E. V., Zhang W., 2006, *ApJ*, 652, 1531
 Radhakrishnan V., Manchester R. N., 1969, *Nature*, 222, 228
 Reichley P. E., Downs G. S., 1969, *Nature*, 222, 229
 Ruderman M., 1969, *Nature*, 223, 597
 Ruderman M., Zhu T., Chen K., 1998, *ApJ*, 492, 267
 Shabanova T. V., 1998, *A&A*, 337, 723
 Shabanova T. V., 2005, *MNRAS*, 356, 1435
 Shabanova T. V., 2007, *Ap&SS*, 308, 591
 Shabanova T. V., 2009, *ApJ*, 700, 1009
 Shabanova T. V., Urama J. O., 2000, *A&A*, 354, 960
 Shemar S. L., Lyne A. G., 1996, *MNRAS*, 282, 677
 Smith D. A., Guillemot L., Camilo F., Cognard I., Dumora D., Espinoza C., Freire P. C. C., Gotthelf E. V., et al. 2008, *A&A*, 492, 923
 Standish E. M., 1998, *JPL Planetary and Lunar Ephemerides*, DE405/LE405, Memo IOM 312.F-98-048. JPL, Pasadena
 Wang N., Manchester R. N., Pace R., Bailes M., Kaspi V. M., Stappers B. W., Lyne A. G., 2000, *MNRAS*, 317, 843
 Wang N., Manchester R. N., Zhang J., Wu X. J., Yusup A., Lyne A. G., Cheng K. S., Chen M. Z., 2001, *MNRAS*, 328, 855
 Zepka A., Cordes J. M., Wasserman I., Lundgren S. C., 1996, *ApJ*, 456, 305
 Zou W. Z., Hobbs G., Wang N., Manchester R. N., Wu X. J., Wang H. X., 2005, *MNRAS*, 362, 1189
 Zou W. Z., Wang N., Manchester R. N., Urama J. O., Hobbs G., Liu Z. Y., Yuan J. P., 2008, *MNRAS*, 384, 1063
 Zou W. Z., Wang N., Wang H. X., Manchester R. N., Wu X. J., Zhang J., 2004, *MNRAS*, 354, 811